Astronomy & Astrophysics manuscript no. aa-1987A-arxiv
November 7, 2012

Letter to the Editor

XMM-Newton observations of SNR 1987A. II. ⋆

The still increasing X-ray light curve and the properties of Fe K lines

P. Maggi[1], F. Haberl[1], R. Sturm[1], and D. Dewey[2]

[1] Max-Planck-Institut für extraterrestrische Physik, Postfach 1312, Giessenbachstr., 85741 Garching, Germany
e-mail: pmaggi@mpe.mpg.de
[2] MIT Kavli Institute, Cambridge, MA 02139, USA

Received 19 October 2012 / Accepted 6 November 2012

ABSTRACT

Aims. We report on the recent observations of the supernova remnant SNR 1987A in the Large Magellanic Cloud with *XMM-Newton*. Carefully monitoring the evolution of the X-ray light curve allows to probe the complex circumstellar medium structure observed around the supernova progenitor star.

Methods. We analyse all *XMM-Newton* observations of SNR 1987A from January 2007 to December 2011, using data from the EPIC-pn camera. Spectra from all epochs are extracted and analysed in a homogeneous way. Using a multi-shock model to fit the spectra across the 0.2–10 keV band we measure soft and hard X-ray fluxes with high accuracy. In the hard X-ray band we examine the presence and properties of Fe K lines. Our findings are interpreted in the framework of a hydrodynamics-based model.

Results. The soft X-ray flux of SNR 1987A continuously increased in the recent years. Although the light curve shows a mild flattening, there is no sudden break as reported in an earlier work, a picture echoed by a revision of the *Chandra* light curve. We therefore conclude that material in the equatorial ring and out-of-plane H ii regions are still being swept-up. We estimate the thickness of the equatorial ring to be at least 4.5×10^{16} cm (0.0146 pc). This lower limit will increase as long as the soft X-ray flux has not reached a turn-over. We detect a broad Fe K line in all spectra from 2007 to 2011. The widths and centroid energies of the lines indicate the presence of a collection of iron ionisation stages. Thermal emission from the hydrodynamic model does not reproduce the low-energy part of the line (6.4–6.5 keV), suggesting that fluorescence from neutral and/or low ionisation Fe might be present.

Key words. ISM: individual objects: SNR 1987A – X-rays: ISM – ISM: supernova remnants – Magellanic Clouds

1. Introduction

SNR 1987A is one of the most studied objects in the southern sky. Because of its location in the Large Magellanic Cloud (LMC) at a distance of 50 kpc, it can be resolved at radio, optical, and even X-ray wavelengths. X-ray observatories such as *ROSAT*, *Chandra* and *XMM-Newton* have frequently observed SNR 1987A, offering a unique opportunity to follow the early evolution of an SNR.

The most important feature of the soft X-ray light curve (between 0.5 and 2 keV) has been the upturn observed about 6 000 days after the explosion (Park et al. 2005), interpreted as the beginning of the interaction of the blast wave with an “equatorial ring” (ER) of denser material around the progenitor star (see for instance Fig. 7 in Sugerman et al. 2002). The ER is likely to have been formed by the interaction between the stellar winds emitted by the progenitor star during its red supergiant and blue supergiant phases (e.g. Chevalier & Dwarkadas 1995), although binary merger models also exist to explain such a structure (e.g. Morris & Podsiadlowski 2007). Monitoring the evolution of the X-ray light curve allows to probe the structure of the ring and to constrain the late stages of the progenitor. Dewey et al. (2012, hereafter D12) presented simple hydrodynamic models that reproduce the soft and hard X-ray light curves; the models show the soft X-ray flux behaviour for both the case where the forward shock has left the ER and the case where the ER is still being shocked (the “thin” and “thick” cases in their Figure 12).

Park et al. (2011, hereafter P11) presented recent *Chandra* observations (up to September 2010). Owing to the apparent flattening of the soft X-ray light curve, these authors concluded that SNR 1987A had reached a new evolutionary phase, where the blast-wave has passed the main body of the ER and is now interacting with matter with a decreasing density gradient. However, Helder et al. (2012, hereafter H12) used the revised ACIS calibration to analyse all *Chandra* observations (including new ones, up to March 2012). They concluded that the sudden break reported by P11 was only a calibration effect.

In this Letter, we present our latest *XMM-Newton* monitoring observations (Sect. 2). We focus first on the evolution of the X-ray flux (Sect. 3), then report the detection of Fe K lines (Sect. 4). Discussion and conclusions are given in Sect. 5.

2. Observations and data reduction

The X-ray photons from SNR 1987A were amongst the first *XMM-Newton* detected in January 2000. This observation and two others from 2001 and 2003 were analysed by Haberl et al. (2006). We then started a yearly monitoring of SNR 1987A, from Januray 2007 (Heng et al. 2008) to December 2011. The high-resolution Reflection Grating Spectrometer (RGS) data taken up to January 2009 are presented in Sturm et al. (2010).

⋆ Based on observations obtained with *XMM-Newton*, an ESA science mission with instruments and contributions directly funded by ESA Member States and NASA.

Table 1. Details of the XMM-Newton EPIC-pn observations

ObsId	Obs. start date	Age [a] (days)	Filter	Total / filtered exp. time [b] (ks)	Flux (0.5–2 keV) $\left(10^{-13}\ \mathrm{erg\,s^{-1}\,cm^{-2}}\right)$	Flux (3–10 keV)	$\dot{F}_X$ [c] (%)
0406840301	2007 Jan 17	7267	Medium	106.9 / 81.9	$33.94^{+0.46}_{-0.49}$	$4.25^{+0.72}_{-0.79}$	—
0506220101	2008 Jan 11	7626	Medium	109.4 / 91.0	$43.76^{+0.47}_{-0.62}$	$5.45^{+0.70}_{-1.45}$	31.1
0556350101	2009 Jan 30	8013	Medium	100.0 / 84.0	$53.05^{+0.61}_{-0.57}$	$6.54^{+0.69}_{-1.62}$	14.3
0601200101	2009 Dec 12	8328	Medium	89.9 / 89.8	$60.09^{+0.61}_{-0.52}$	$7.82^{+0.57}_{-1.34}$	31.2
0650420101	2010 Dec 12	8693	Medium	64.0 / 61.7	$66.91^{+0.87}_{-0.90}$	$9.32^{+0.74}_{-1.57}$	11.3
0671080101	2011 Dec 02	9048	Medium	80.6 / 70.5	$71.88^{+0.48}_{-0.70}$	$11.31^{+0.66}_{-1.82}$	10.5

Notes. Fluxes are given with 3σ errors (99.73 % C.L.). [(a)] Number of days since the explosion of SN 1987A. [(b)] Total and useful (filtered) exposure times, after removal of high background intervals. [(c)] Increase rate in % since previous measurement, normalised to one year.

Here we homogeneously (re-)analyse all observations from 2007 to 2011, three of which have not been published so far. We mainly use data from the EPIC-pn camera (Strüder et al. 2001), operated in Full-Frame mode with medium filter. Details of the observations are listed in Table 1. We processed all observations with the SAS[1] version 11.0.1. We extracted spectra from a circular region centered on the source, with a radius of 25″. The background spectra were extracted from a nearby point source-free region common to all observations. We selected single-pixel events (`PATTERN = 0`) from the pn detector. We rebinned the spectra with a minimum of 20 counts per bin in order to allow the use of the χ^2-statistic. Non-rebinned spectra were used with the C-statistic (Cash 1979) for the study of Fe K lines (see Sect. 4), because of the limited photon statistics above 6 keV. The spectral fitting package XSPEC (Arnaud 1996) version 12.7.0u was used to perform the spectral analysis.

3. X-ray light curve

To measure the X-ray flux of SNR 1987A, we fitted the EPIC-pn spectra with a three-component plane-parallel shock model (called vpshock in XSPEC, where the prefix "v" indicates that abundances can vary), using `neivers` 2.0. This is the same model as the one used by D12 for *Chandra* and *XMM-Newton* spectra, with a fixed-temperature component ($kT = 1.15$ keV), although we did not use a Gaussian smoothing. This model gives slightly better fits than when using a two-component model(*e.g.* Park et al. 2004; Heng et al. 2008). The high and low-temperature components are believed to originate from the interaction of the shocks with uniform material and denser clumps in the ER, respectively (D12). Another interpretation is that the high-temperature component comes from plasma shocked a second time by a reflected shock (Zhekov et al. 2006).

For elemental abundances, we followed the same procedure as in Haberl et al. (2006): N, O, Ne, Mg, Si, S and Fe abundances were allowed to vary but were the same for all observations, whereas the He, C, Ar, Ca and Ni abundances were fixed. The systemic velocity of SNR 1987A (286 km s^{-1}, *e.g.* Gröningsson et al. 2008) was taken into account by choosing the redshift accordingly.

For the absorption of the source emission, we included two photoelectric absorption components, one with $N_{H\ \mathrm{Gal}} = 0.6 \times 10^{21}$ cm^{-2} (fixed) for the Galactic foreground absorption (Dickey & Lockman 1990) and another one with $N_{H\ \mathrm{LMC}}$ (free in the fit) for the LMC. Metal abundances for the second absorption component are fixed to the average metallicity in the LMC (*i.e.*, half the solar values, Russell & Dopita 1992). All spectra share the same $N_{H\ \mathrm{LMC}}$.

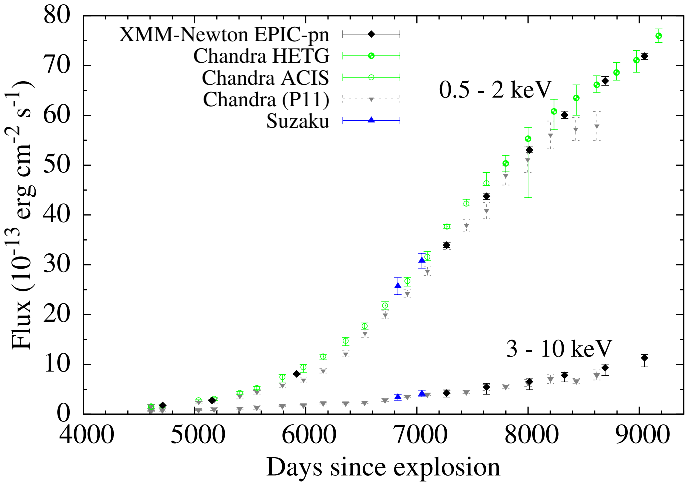

Fig. 1. Light curve of SNR 1987A in the soft and hard X-ray ranges. *XMM-Newton* data points (black diamonds) after day 7000 are given with 99.73 % C. L. error bars. Updated *Chandra* measurements ((with 68 % C. L. errors, H12) and those based on the older calibration (with 90 % C. L. errors, P11) are shown in green and gray, respectively. Suzaku measurements (Sturm et al. 2009, blue triangles) are also shown.

We simultaneously fitted the six spectra using energies between 0.2 and 10 keV. For consistency with the detection of Fe K lines (see Sect. 4), we included an additional (Gaussian) line to the model for the spectra obtained after 2007. The central energies and widths of the lines were fixed to the values found in the detailed analysis (Sect. 4). Only the normalisation of each line was let free.

The fit was satisfactory, with $\chi^2 = 4125.06$ for 3443 degrees of freedom. Although detailed spectral fits are not the focus of this study, we found that *(i)* the best-fit $N_{H\ \mathrm{LMC}}$ was $3.09^{+0.07}_{-0.08} \times 10^{21}$ cm^{-2}, corresponding to a total absorption column of 3.7×10^{21} cm^{-2}, somewhat higher than found using the grating instruments aboard *Chandra* and *XMM-Newton* (Sturm et al. 2010; Zhekov et al. 2006), *(ii)* the abundance pattern is in line with the one reported by Sturm et al. (2010) and D12, *(iii)* the temperature of the cool component increased only slightly from 0.34 to 0.38 keV, while its normalisation remained constant, and *(iv)* the temperature of the hot component is always in

[1] Science Analysis Software, `http://xmm.esac.esa.int/sas/`

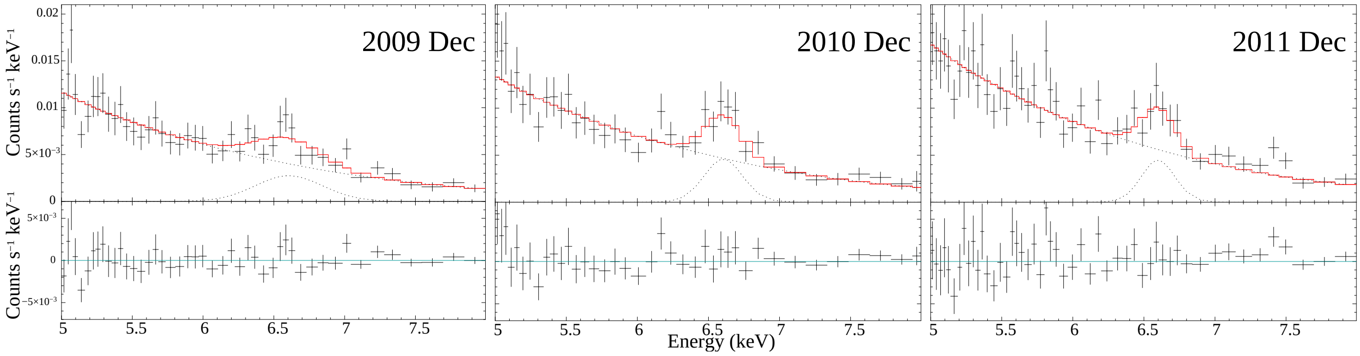

Fig. 2. Recent EPIC-pn spectra of SNR 1987A in the 5–8 keV range, showing the Fe K lines. The model used (red) is the sum of two components: a bremsstrahlung continuum and a Gaussian, shown by dotted lines. The bottom panels show the fit residuals. All panels have the same scale. Note that for plotting purpose only, adjacent bins are rebinned in order to have a significant ($\geq 5\sigma$) detection in each rebinned channel. The feature seen at ~7.4 keV in the 2011 spectrum is an instrumental artefact and not a Ni K line.

excess of 3.5 keV, and its normalisation and contribution steadily increased.

We measured the soft (0.5–2 keV) and hard (3–10 keV) fluxes at all epochs, using the XSPEC `flux` command. We list the results, with 3σ uncertainties (99.73 % confidence level, C. L.) in Table 1. Note that as customary for SNR 1987A we give *absorbed* fluxes, so comparisons between various obser-vatories are easier (because they do not depend on the column densities obtained from the fit). The fluxes up to January 2009 are fully consistent with the results from Heng et al. (2008) and Sturm et al. (2010) which used the same data.

We included these results in the X-ray light curve shown in Fig. 1. Older *XMM-Newton* fluxes are taken from Haberl et al. (2006). We show the *Chandra* measurements with the old calibration (P11) and the newest one (H12). We also add the results from Suzaku observations (Sturm et al. 2009).

Within their respective errors, *XMM-Newton*, *Chandra*, and Suzaku measured soft and hard X-ray X-ray fluxes which agree very well. P11, using the ACIS calibration available at that time, stated that the soft X-ray flux from SNR 1987A has been nearly constant after day ~ 8000. Obviously *XMM-Newton* observed a source that was *not* constant, although we do observe a mild flattening of the light curve. The increase rates of the soft X-ray flux (last column of Table 1) vary from one year to another, showing that the evolution of the X-ray flux is not smooth. One should therefore be cautious when claiming a steepening or flattening of the light curve and wait for a longer baseline.

The discrepancy between *Chandra* and *XMM-Newton* measurements after day 8000 is reconciled by H12, using the revised *Chandra* calibration. They concluded that the apparent break in the soft X-ray light curve (P11) was mainly due to build-up of contamination on the ACIS optical blocking filters.

4. Fe K lines

The superior high-energy effective area of *XMM-Newton* (~ 900 cm^{-2} at 6.4 keV *vs.* ~ 200 cm^{-2} for *Chandra*) allows the study of Fe K lines with the EPIC cameras, at energies between 6.4 and 6.7 keV, *i.e.* out of the range covered by RGS. Heng et al. (2008) noted a possible detection of an Fe Kα line in the spectrum obtained in 2007, but the insufficient statistics precluded a more detailed analysis. In the coadded spectra from 2007 to January 2009, Sturm et al. (2010) identified a line at 6.57 ± 0.08 keV.

We analysed the presence and properties of Fe K lines in all the monitoring observations (Table 1). We fitted the non-rebinned spectra with a bremsstrahlung continuum and a Gaussian line, making use of the C-statistic to take into account the limited number of counts in each bin. We performed *F-tests* to evaluate the significance of the line in each observation: we found a detection more than 3σ (respectively 4σ) significant in the data from 2008 and 2011 (respectively December 2009 and 2010). The January 2009 observation, having a slightly shorter exposure due to longer high background activity periods, still yields a 2σ detection. We found only a marginal (1σ) detection in the 2007 spectrum, in agreement with previous studies.

Table 2. Fe K line properties.

Epoch	$E_{\rm line}$ (keV)	σ-width (eV)	Flux (10^{-6} ph cm^{-2} s^{-1})	EW (eV)
2008 Jan	$6.58^{+0.05}_{-0.07}$	46 (< 146)	$1.07^{+0.57}_{-0.46}$	174
2009 Jan	$6.55^{+0.15}_{-0.14}$	125 (< 433)	$0.94^{+1.50}_{-0.65}$	169
2009 Dec	$6.63^{+0.11}_{-0.09}$	229 (< 424)	$2.64^{+1.69}_{-1.78}$	432
2010 Dec	$6.61^{+0.06}_{-0.06}$	105 (< 227)	$2.51^{+1.39}_{-0.99}$	344
2011 Dec	$6.61^{+0.06}_{-0.06}$	83 (< 178)	$2.08^{+1.01}_{-0.86}$	238

Notes. Central energy, σ-width, total photon flux and equivalent width (EW) of the Gaussian used to characterise the Fe K feature in the spectra of SNR 1987A. We give 90 % C. L. errors.

We show the lines in the three unpublished spectra in Fig. 2. The plasma temperatures of the bremsstrahlung continua range from kT = 2.75 to 3 keV, and the emission measures follow the increasing trend of the hard X-ray flux. Line properties are given in Table 2 for all observations except the one from 2007.

No evolution of the line central energy is found within the uncertainties, but our spectra suffer from limited statistics. The energy of the Fe K line depends on the ionisation stage of iron, increasing from 6.4 keV for Fe II, to 6.7 keV for Fe XXV (Makishima 1986; Kallman et al. 2004). The spectral resolution is only ~ 160 eV (Strüder et al. 2001), so we are not able to resolve possible contributions from different Fe ions present in the X-ray emitting plasma. Therefore, the large measured widths of the lines in our spectra are most likely a sum of lines (which might be Doppler-broadened) from several Fe ions, convolved with the instrumental response of the camera. The weighted average of the emission-line centroids (6.60 ±0.01 keV) and the typical widths (~ 100 eV) indicate the presence of ionisation stages from Fe XVII to Fe XXIV. This is consistent with the detection of lines from Fe XVII to Fe XX in the RGS

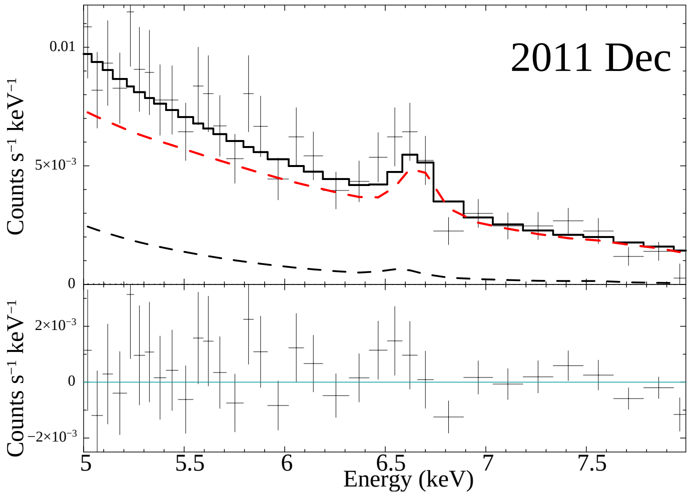

Fig. 3. Details of the Fe K lines region of the spectrum from December 2011. The model used is the three-shock components model described in Sect. 3, including emission from Fe below He-like ions and without a Gaussian line. The "hot" component (red dashed line) dominates the continuum and line spectrum but does not account for an emission excess around 6.55 keV.

spectra (Sturm et al. 2010), and the detection of a Fe XXII–Fe XXIII blend in the *Chandra* High Energy Transmission Grating spectra (Dewey et al. 2008).

The flux in the iron line indicates an increase around day 8000, and a decrease afterwards. However, given the large (statistical) errors in the flux measurements, we cannot exclude the possibility that the flux of the line remained constant in the last three years. Since the hard continuum steadily increased during that period of time, the equivalent width of the line decreased in the last observations (Table 2).

5. Discussion and Conclusions

Our monitoring campaign with *XMM-Newton* since 2007 is ideally suited to follow the evolution of SNR 1987A: *(i)* we used the same intrument setting (observing mode, filter, readout time); *(ii)* we extracted the spectra in the same regions and *(iii)* we used the same model for all the spectra. The high throughput of *XMM-Newton* results in a high statistical quality of our spectra. This allows high-confidence flux measurements with relatively small errors and free of cross-calibration issues due to different observing modes.

Our light curve shows a continuous increase of the soft X-ray flux of SNR 1987A, indicating that no turn-over has been reached yet and that the blast wave is still propagating into dense regions of the ER. To further constrain the thickness of the ER, given the continuous increase of the soft X-ray flux, we use the "2×1D" hydrodynamical model from D12. The recent *XMM-Newton* and *Chandra* measurements point towards a thickness of at least 4.5×10^{16} cm (0.0146 pc) for the ER, and each year of continued flux increase requires an additional ER thickness of $\sim 0.53 \times 10^{16}$ cm (0.0017 pc).

The high-energy collective power of *XMM-Newton* allows us to detect and characterise the Fe K lines from SNR 1987A. We find that the energies and the widths of the lines imply the presence of a collection of ionisation stages for iron. To investigate which model component is most responsible for the Fe K lines, we use the best-fit three-shock model (switching off the Gaussian line) and using the NEI version 1.1, as it includes low ionisation stages (below He-like ions), which allows to probe the whole range of energy between 6.4 and 6.7 keV as function of kT and τ (see Fig. 3 in Furuzawa et al. 2009). As expected, we find that only the high-temperature component significantly contributes to the hard continuum and the line. When including emission from ions below He-like iron, the shapes and fluxes of the lines from the high-temperature component (Fig. 3) fail to reproduce the data. There is need for lower ionisation stages to explain the excess observed at ~6.55 keV. This points to the presence of shocked material with shorter ionisation ages τ. In the framework of the hydrodynamics-based model from D12, we find that the main contribution to the Fe K emission therefore comes from the out-of-plane material ("H II region"), which has temperature and ionisation age producing emission in the 6.55–6.61 keV range. Another possibility for the low-energy emission (~ 6.4 keV) is fluorescence from near-neutral Fe, including Fe in the unshocked ejecta. Material in the dense ER clumps, on the other hand, has a temperature too low to significantly contribute to the line.

Following the evolution of the Fe K line fluxes and centroid energies is crucial to constrain their origin. Next-generation instrumentation, such as the X-ray calorimeter aboard Astro-H will be able to resolve lines from different Fe ions, thus providing even deeper physical insights.

The calibration issues encountered by the *Chandra* team show how important it is to use *both* observatories to monitor such an important source. To follow the evolution of the light curve and of the iron lines, subsequent observations of SNR 1987A with *XMM-Newton* are highly desired.

Acknowledgements. The *XMM-Newton* project is supported by the Bundesministerium für Wirtschaft und Technologie / Deutsches Zentrum für Luft- und Raumfahrt (BMWi/DLR, FKZ 50 OX 0001) and the Max-Planck Society. P. M. and R. S. acknowledge support from the BMWi/DLR grants FKZ 50 OR 1201 and FKZ 50 OR 0907, respectively.

References

Arnaud, K. A. 1996, in Astronomical Society of the Pacific Conference Series, Vol. 101, Astronomical Data Analysis Software and Systems V, ed. G. H. Jacoby & J. Barnes, 17
Cash, W. 1979, ApJ, 228, 939
Chevalier, R. A. & Dwarkadas, V. V. 1995, ApJ, 452, L45
Dewey, D., Dwarkadas, V. V., Haberl, F., Sturm, R., & Canizares, C. R. 2012, ApJ, 752, 103
Dewey, D., Zhekov, S. A., McCray, R., & Canizares, C. R. 2008, ApJ, 676, L131
Dickey, J. M. & Lockman, F. J. 1990, ARA&A, 28, 215
Furuzawa, A., Ueno, D., Hayato, A., et al. 2009, ApJ, 693, L61
Gröningsson, P., Fransson, C., Leibundgut, B., et al. 2008, A&A, 492, 481
Haberl, F., Geppert, U., Aschenbach, B., & Hasinger, G. 2006, A&A, 460, 811
Helder, E. A., Broos, P. S., Dewey, D., et al. 2012, submitted to ApJ
Heng, K., Haberl, F., Aschenbach, B., & Hasinger, G. 2008, ApJ, 676, 361
Kallman, T. R., Palmeri, P., Bautista, M. A., Mendoza, C., & Krolik, J. H. 2004, ApJS, 155, 675
Makishima, K. 1986, in Lecture Notes in Physics, Berlin Springer Verlag, Vol. 266, The Physics of Accretion onto Compact Objects, ed. K. O. Mason, M. G. Watson, & N. E. White, 249
Morris, T. & Podsiadlowski, P. 2007, Science, 315, 1103
Park, S., Zhekov, S. A., Burrows, D. N., Garmire, G. P., & McCray, R. 2004, ApJ, 610, 275
Park, S., Zhekov, S. A., Burrows, D. N., & McCray, R. 2005, ApJ, 634, L73
Park, S., Zhekov, S. A., Burrows, D. N., et al. 2011, ApJ, 733, L35
Russell, S. C. & Dopita, M. A. 1992, ApJ, 384, 508
Strüder, L., Briel, U., Dennerl, K., et al. 2001, A&A, 365, L18
Sturm, R., Haberl, F., Aschenbach, B., & Hasinger, G. 2010, A&A, 515, A5
Sturm, R., Haberl, F., Hasinger, G., Kenzaki, K., & Itoh, M. 2009, PASJ, 61, 895
Sugerman, B. E. K., Lawrence, S. S., Crotts, A. P. S., Bouchet, P., & Heathcote, S. R. 2002, ApJ, 572, 209
Zhekov, S. A., McCray, R., Borkowski, K. J., Burrows, D. N., & Park, S. 2006, ApJ, 645, 293